SEX-SPECIFIC BONE PHENOTYPE IN THE STREPTOZOTOCIN-INDUCED MURINE MODEL OF DIABETES

by

Jennifer Hatch

A Thesis

Submitted to the Faculty of Purdue University

In Partial Fulfillment of the Requirements for the degree of

Master of Science in Biomedical Engineering

Department of Biomedical Engineering

Indianapolis, Indiana

August 2021

THE PURDUE UNIVERSITY GRADUATE SCHOOL
STATEMENT OF COMMITTEE APPROVAL

Dr. Joseph M. Wallace, Chair

Department of Biomedical Engineering

Dr. Matthew R. Allen

Department of Anatomy, Cell Biology, and Physiology
Indiana University School of Medicine

Dr. Robert N. Bone

Department of Pediatrics
Indiana University School of Medicine

Dr. Jiliang Li

Department of Biology

Dr. Sungsoo Na

Department of Biomedical Engineering

Approved by:

Dr. Joseph M. Wallace

To Adam:

Thank you for being my support for 5 years while I went off to college. This was never what you signed up for and I love you for continuing to love me, feed me, and fold countless loads of laundry along the way.

To Sabria:

In coming back to college, I never imagined I would make the sort of life-long friend who would be happy to endlessly discuss with me all the big questions about life, love, God, math, politics, ethics and the endless list of silly little things we have filled the time with in between. Thank you for your friendship, your insight, and for always finding my missing negative signs!

To my parents and my kids:

Thank you for never doubting for a second that I could succeed, even when I didn't believe it myself, and thank you for the time you gave me and let me take from you so that I could follow my dreams. I love you to the moon and stars and back.

ACKNOWLEDGMENTS

I would like to extend a special thanks to my thesis committee for their expert advice and endless patience during this project, to Dr. Robert Considine at Indiana University School of Medicine for development of a protocol to measure glycated hemoglobin in mice and to Dr. Corinne Metzger for the help and guidance on blood collection. Additional thanks go to all of my fellow lab members at the Bone Biology and Mechanics Lab for their help and advice along the way.

TABLE OF CONTENTS

LIST OF TABLES

LIST OF FIGURES

LIST OF ABBREVIATIONS

ADA	American Diabetes Association
AGE	Advanced Glycation End Product
BA	Cortical Bone Area
BG	Blood Glucose
BMD	Bone Mineral Density
BV/TV	Bone Volume Fraction
CML	N(Carboxymethyl)lysine
Ct. Th.	Cortical Thickness
ER	Endoplasmic Reticulum
ERα	Estrogen Receptor Alpha
ERβ	Estrogen Receptor Beta
FPG	Fasting Plasma Glucose
GluOCN	Uncarboxylated Osteocalcin
GPER	G-Protein Coupled Estrogen Receptor
GTT	Glucose Tolerance Test
HbA1c	Hemoglobin A1c
IDF	International Diabetes Foundation
ITT	Insulin Tolerance Test
MSC	Mesenchymal Stem Cell
NK	Natural Killer Cell
NOD	Non-Obese Diabetic Mouse
OB	Osteoblast
OC	Osteoclast
PBS	Phosphate Buffered Saline
PTH	Parathyroid Hormone
RAGE	Receptor for Advanced Glycation End Products
ROS	Reactive Oxygen Species
SMI	Structure Model Index
SOST	Sclerostin

STZ	Streptozotocin
T1D	Type 1 Diabetes Mellitus
T2D	Type 2 Diabetes Mellitus
TA	Total Cross-sectional Area
Tb. N	Trabecular Number
Tb. Sp	Trabecular Separation
Tb. Th	Trabecular Thickness
TMD	Tissue Mineral Density
TMD	Total Mineral Density
μCT	Microcomputed Technology

ABSTRACT

Bone disease and degradation is a ubiquitous problem, the complexity and treatment of which humanity has only begun to understand. Diabetes Mellitus is a disease which, in all forms, profoundly effects the organs of the body, bone included. As is often the case in biology, there are inherent differences between the sexes when considering skeletal development and disease progression and outcome. Although there are several reported mouse models for diabetes, until now there has been no characterization of bone disease in any model where diabetes occurs with equal frequency in males and females in greater than 90% of animals. In this study, a protocol for reliable induction of diabetes in both sexes using intraperitoneal injections of Streptozotocin was developed. The resulting bone phenotype in male and female mice was characterized and compared to weight and age matched control groups. In this model female diabetic mice exhibited a robust deficit in bone quality, while both sexes experienced loss of beta-cell mass and increased glycation of hemoglobin rendering the diabetic mice unable to produce insulin endogenously. Further, these mice were unable to metabolize exogenous insulin injected during insulin tolerance testing. This model is a strong candidate for future exploration of osteoporotic bone disease, Diabetes Mellitus, and the link between estrogen and glucose sensitivity.

1. INTRODUCTION

The recorded history of humans practicing medicine leans as far back in time as 3000 B.C., and though Hippocrates is credited with saying *"One should first get a knowledge of the structure of the spine; for this is also requisite for many diseases"* around 400 B.C., his belief was that the spine existed solely to hold the body erect and give shape to the human form [1, 2]. By the mid 1800's it was understood that marrow was a key location for the production of blood, but it wasn't until the 1950's that bone became widely recognized as a regulator of mineral homeostasis in the body [3]. In fact, it is only within the last 15 years, that bone has begun to be understood as the powerful endocrine organ that it is. Although bone only makes up an estimated 15% of a body's mass, the extensive surface area of the bone within the body, the highly vascularized network of channels running through the bone, and the perfusion of the marrow cavities within the long bones makes bone a frequent participant in chemical and hormonal signaling [4]. Bone loss occurs with age, particularly in women, as well as from many other causes, a list of which is enumerated in **Table 1**. Over two thousand years later, is now clear that Hippocrates was more correct than he ever imagined: knowledge of the bone is indeed a requisite for understanding disease.

Mechanically, bone is a triphasic composite material consisting of the mineral hydroxyapatite ($Ca_{10}(PO_4)_6(OH)_2$, 60%), organic proteins (mainly type-I collagen, 30%) and water (10%) [5]. The maintenance of healthy bone requires a constant coupled remodeling process whereby bone is dissolved by osteoclasts (OCs) and replaced by osteoblasts (OBs). This continuous process of bone resorption and deposition occurs in response to paracrine signaling within the bone. The complex signaling system may be coopted, as in the case of tumor growth, or dysregulated, as in the case of menopause. Current methods of treatment involve mechanical loading through exercise and use of drugs such as bisphosphonates, raloxifene, zoledronic acid, gastro-resistant risedronate, and teriparatide [6]. None of these drugs present a cure, and the quest to understand the complicated signaling mechanisms involved in the regulation of bone remodeling and mitigate the symptoms of altered remodeling in disease is ongoing. Additionally, the dynamic nature of bone means that it is constantly interacting in complicated patterns with the rest of the body (**Figure 1**).

Table 1. Many causes of osteoporosis. This non-exhaustive list provides a look at the pervasive nature of bone disease as a secondary symptom. [7].

Genetic Disorders	Ehlers-Danlos, Glycogen storage diseases, Gaucher disease, Hemochromatosis, Homocystinuria, Hypophosphatasia, Marfan syndrome, Menkes steely hair syndrome, Osteogenesis imperfecta, Porphyria, Riley-Day syndrome
Hypogonadal States	Androgen insensitivity, Anorexia nervosa/bulimia, Athletic amenorrhea, Hyperprolactinemia, Panhypopituitarism, Premature menopause, Turner and Kleinfelter syndromes
Endocrine Disorders	Acromegaly, Adrenal insufficiency, Cushing syndrome, Diabetes mellitus, Hyperparathyroidism (1 and 2), Thyroid disease
Gastrointestinal Diseases	Gastrectomy, Inflammatory bowel disease, Malabsorption, Celiac disease, Primary biliary cirrhosis
Hematologic Disorders	Sickle cell disease, Thalassemia, Hemophilia, Multiple myeloma, Leukemias and lymphomas, Systemic mastocytosis
Rheumatologic Diseases	Ankylosing spondylitis, Rheumatoid arthritis
Nutritional Deficiencies	Calcium, Magnesium, Vitamin D
Drugs	Anticoagulants (heparin and warfarin), Anticonvulsants, Cyclosporines and tacrolimus, Cytotoxic drugs, Glucocorticoids (and adrenocorticotropic hormone), Gonadotropin-releasing hormone agonists, Methotrexate, Thyroxine
Miscellaneous	Alcoholism, Amyloidosis, Chronic metabolic acidosis, Congestive heart failure, Cystic fibrosis, Emphysema, End stage renal disease, Idiopathic hypercalciuria, Idiopathic scoliosis, Immobilization, Multiple sclerosis, Organ transplantation, Parenteral nutrition, Sarcoidosis

Sexual dimorphism is a common feature of organ systems and bone is no exception. These differences in development and chemical interactions of the bone are driven by sex hormones and although androgens play an important role in bone physiology, researchers have shown that it is the presence of estrogen that controls the dimorphic features in the skeleton [8]. In animals, each class of hormones is produced and utilized to varying degrees, the ratio of which contributes greatly to our understanding of an organism as biologically male or female. These

differences often lead to a divergence in the presentation and progression of disease and may alter the efficacy of treatment. As such, development of comprehensive animal models for the study of human disease requires consideration of both sexes. Additionally, as medicine begins to recognize the growing body of individuals undergoing hormone therapy, a deeper understanding will be needed of how estrogens and androgens interact with the body in various disease states and the ways in which they may contribute to or complicate treatment of disease.

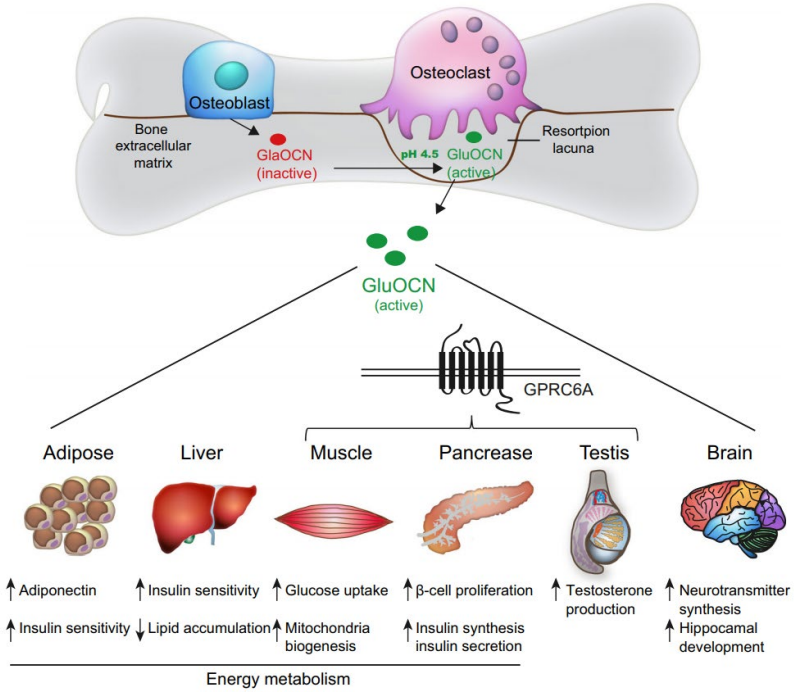

Figure 1. Interaction of bone with organs throughout the body. Beyond sending paracrine signals throughout the bone, bone cells are involved in endocrine signaling with many organs and tissue types throughout the body. There is a strong relationship between undercarboxylated osteocalcin (GluOCN) and the bodily system of insulin synthesis, secretion, and sensitivity. [4].

Diabetes mellitus is one such disease in which rate of incidence, rate of disease progression, and overall disease phenotype differ between sexes. Characterized as an inability to regulate and/or process insulin, diabetes mellitus affected an estimated 6.4% of adults as of 2010, with that number expected to rise to 7.7% of the world's adult population by 2030 [9]. Insulin is a hormone produced by pancreatic islet β-cells which stimulates glucose uptake and regulates the bodily storage of carbohydrates and lipids [10]. Diabetic patients are at a higher risk of bone fracture at all stages of life due to reduced bone mineral density and altered cell repair cycles [11, 12].

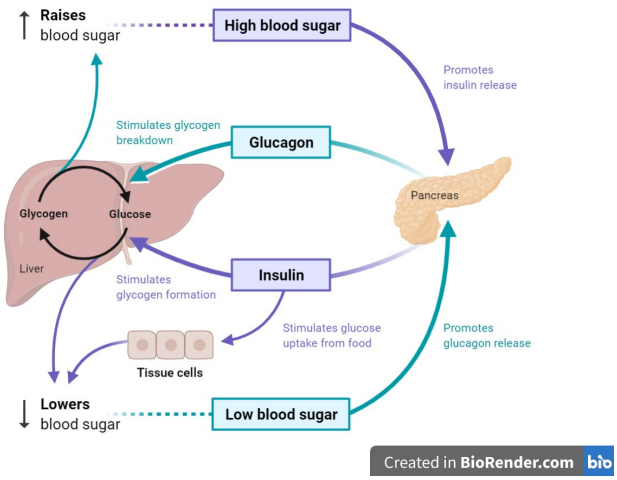

Figure 2. Metabolism of glucose. Glucose in the bloodstream signals the pancreas to produce insulin which stimulates the uptake of glucose by cells for conversion to ATP and storage as glycogen. When glucose levels drop, the pancreas produces glucagon which triggers the conversion of the stored energy to glucose which will then be converted to ATP.

The two most common forms of diabetes mellitus are type 1 diabetes (T1D) and type 2 diabetes (T2D). Type I Diabetes is a polygenic disorder, although genetic abnormality does not guarantee that disease will develop [13]. Onset of disease involves a trigger event which may be random, induced by viral infection such as the enterovirus, or some other unknown mechanism. Triggers vary from case to case, and likely do not have a direct effect on disease severity [13]. The trigger event induces an immune response with CD8+ T lymphocytes playing a key role, and CD4+ T cells playing a secondary role in attacking the β-cells native to the islet of Langerhans in the pancreas [13]. Type I diabetes is generally diagnosed during a period where the patient may still have some β-cell function, and frequently these patients may see an immediate improvement in symptoms when treatment begins. Over time, loss of function of β-cells may become complete although some patients retain residual β-cells decades after disease onset [13]. Absent the ability of the β-cells to produce insulin, the body has no adequate system to regulate glucose levels in the blood.

Consistently elevated blood glucose leads to a variety of bodily symptoms. In children, T1D causes polydipsia, polyuria, weight-loss, and diabetic ketoacidosis [13]. Children with T1D are more likely to be hospitalized, to have thyroid disease, colitis, cardiovascular disorders, suffer from mental disorders, epilepsy, and pulmonary disease than their age-matched peers [14]. Daily treatment with exogenous insulin becomes necessary as the loss of β-cell function becomes

complete. In adults, which comprise up to 50% of newly diagnosed T1D cases each year, symptoms may be less traditional or may be mistaken for Type 2 Diabetes [15].

T2D is characterized as a metabolic disorder in which the body develops insulin resistance over time, leading to obesity, hypertension, and cardiovascular complications. However, some patients do not fit into either category. In the early 1990's researchers began to recognize a subset of insulin deficient T1D patients who later developed insulin resistance as well. These patients are characterized by an autoimmune response to the β-islet cells, obesity, and resistance to insulin treatment and the prevalence within the diabetic community may be as high as 30% [9, 16]. Both the prevalence of diabetes and the inability to fit patients into neatly understood categories underscore the need for more research into the mechanisms underlying the disease and potential treatments for common symptoms.

In 2018, the International Diabetes Foundation (IDF) reported on data compiled from researchers in Africa, Europe, the Middle East and North Africa, North America and the Caribbean, South and Central America, South-East Asia and the Western Pacific, finding that differences in diabetes prevalence can be correlated with age group, World Bank income group, geographical region, and sex. Diabetes was roughly three times more common in wealthier populations, and the peak prevalence occurred in older individuals, while globally men outpaced women in the diabetic population at a ratio of 1.06:1. In men, the peak prevalence occurred around 60-69 years of age compared with around 70-79 years of age in women, and in some regions the ratio of male to female within the diabetic population was as high as 1.42:1 [17].

There is a sexual dimorphism in the energy partitioning of males and females, with females possessing a greater ability to store energy as fat, though no difference in energy expenditure has been observed between the sexes which may be due to the increased ratio of brown to white adipocytes in females vs. males [18-20]. As the female body approaches menopause, the risk of metabolic disorder increases as visceral fat is more easily stored around muscles [19]. Work with mouse models attempting to parse the influence of the X and Y chromosomes has shown that increasing the number of X chromosomes correlates to an increase in propensity for fat storage, while the presence of the Y chromosome correlates to a lower ability to metabolize glucose [18, 21]. While the relative proportions of androgens to estrogens are important in these systems, it has been well documented that it is the estrogens which confer the protective effects against insulin resistance and altered glucose metabolism [22].

Estrogens protects pancreatic β-cells from apoptosis and prevent insulin-deficiency in mice [23]. Estrogen signaling is regulated through three main receptors: estrogen receptor alpha (ERα), estrogen receptor beta (ERβ), and the G-protein-coupled estrogen receptor (GPER). Of these receptors, ERα is the most consequential in the activity of estrogen within the pancreas, protecting β-cells from apoptosis and modulating mitochondrial activity [40]. At menopause, this protection is reduced not only in the pancreas but throughout the body. However, the endocrine functions of estrogen in the reproductive system make it a poor target for therapy.

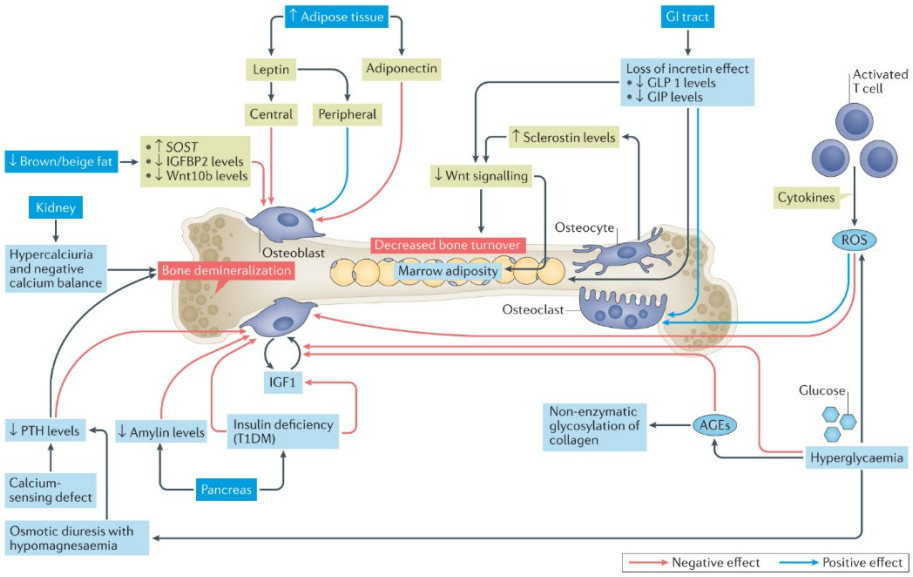

Figure 3. The many-faceted effects of diabetes on bone. AGEs directly affect the structural properties of bone while also reducing the number of available cells responsible for the bone modeling process. Bone mineral density is reduced through loss of calcium and vitamin D [24].

During the extended periods of hyperglycemia in which hemoglobin becomes glycated, the surplus glucose in the body also reacts with proteins and lipids to form advanced glycation end products (AGEs). This non-enzymatic binding reaction between sugars and proteins, lipids, or nucleic acids form within the bone, reducing the capability of the bone to absorb energy without fracturing (**Figure 3)** [25, 26]. AGEs may induce apoptosis of mesenchymal stem cells (MSCs), reducing the number of cells available to become osteoblasts [26, 27]. Two AGEs commonly found in bone are pentosidine and N(carboxymethyl)lysine (CML), the development of which accelerates with the progression of diabetes and prolonged hyperglycemia [28]. In differentiated cells, AGEs activate the receptor for AGEs (RAGE) leading to inflammation which signals the

osteoclasts to increase the rate of bone resorption [24]. The overactive OCs increase serum levels of sclerostin (SOST), a Wnt/β-catenin inhibitor which leads to fewer osteoblasts and an inability to repair damaged bone [29] Additionally, the hypercalciuric state of diabetic patients creates a net-negative balance of calcium in the body [30]. Reduced calcium levels signal the parathyroid glands to release parathyroid hormone (PTH) which further stimulates bone resorption as the body attempts to stabilize serum calcium levels by liberating calcium stored in the skeleton [31]. Vitamin D deficiency, also frequently seen in diabetic patients, further accelerates this bone loss as Vitamin D plays a compensatory role in the maintenance of bone mineral density (BMD) in low-calcium states [1] . The net result is the clinical association of diabetes with decreased bone mineral density (BMD) in T1D patients, a smaller cross-sectional area in the radius and tibia, increased cortical porosity, and bones that fail in brittle fracture [24].

Historically, diagnosis of Diabetes Mellitus relied on measurements of blood glucose (BG) or fasting plasma glucose (FPG). Current recommendations by the American Diabetes Association (ADA) prefer the use of Hemoglobin A1c (HbA1c) as a marker for diagnosis. The percentage of HbA1c in the blood serum measures the non-enzymatic glycation of hemoglobin [32]. Studies of HbA1c levels between sexes demonstrate that diabetic females tend to have a higher percentage of glycated cells although men were more sensitive to the increased blood glucose at lower levels [33, 34]. The differences between disease progression and presentation in males and females highlight the need for consideration of both sexes in pre-clinical research. As such, any dimorphism exhibited in animal models should be carefully considered.

Animal models of diabetes offer the opportunity to study the effects of diabetes on the body. To look at the effects of diabetes on bone it is important to use a model that will emulate the disease state for a period of time sufficient for the development of bone disease. Four types of mouse models were used to model Type 1 diabetes: autoimmune, genetically induced, viral, and chemical. The genetically induced AKITA mouse model for T1D develops diabetes around 3 – 4 weeks of age. The model carries a monogenic mutation in the insulin 2 gene which leads to a protein misfolding causing endoplasmic reticulum stress-induced hyperglycemia [35]. The age of diabetes onset makes this mouse a candidate for study of juvenile diabetes, but the effects of insulin treatment in these mice may alter the bone phenotype making it an undesirable candidate for study of diabetic effects on bone.

The non-obese diabetic mouse (NOD) is another model for T1D which requires treatment with insulin for survival. In this autoimmune model disease begins around 3-4 weeks of age when lymphocytic CD4+ and CD8+ T cells, B cells and natural killer cells (NK cells) begin to attack the pancreatic islet cells, however, onset of diabetes does not occur until after 15 weeks of age [36]. This mechanism of induction is highly conserved with human development of T1D, however complete loss of insulin production is not guaranteed. Incidence of diabetes is dimorphic and occurs in 60%-90% of females and 10%-30% of males [35]. A second downside of this model is that mice reach equivalent adult age before diabetes is induced, making it impossible for use in the study of bone development.

In viral models, scientists exert a controlled attack of the β-cell islet, but these models are reliant on the viral load and rate of replication [35]. Additionally, the complications of viral use in research and the unreliable rate of disease development are downsides to the use of these models.

Models that use chemicals to destroy the β-islet have been used since the 1960's, and the two most commonly used chemicals are Alloxan and Streptozotocin (STZ) which are both similar in structure to glucose, leading to competitive inhibition with normal glucose regulation (**Figure 4**). Alloxan is an unstable chemical which causes diabetes by inhibiting insulin secretion and promoting the formation of reactive oxygen species (ROS) which lead to β-cell death, although the insulin inhibition is easily reversed making the hyperglycemic state difficult to control [37]. The accurate dosing range of alloxan is narrow while the systemic toxicity is not-easily managed, making alloxan a difficult drug to use in controlled studies [35]. STZ is an unstable antibiotic, but the reduced systemic toxicity allows for a wider dosing range than alloxan.

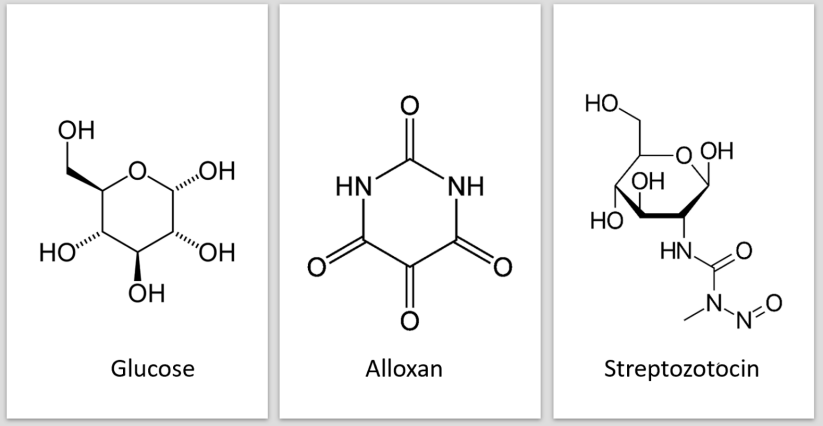

Figure 4. The structures of glucose, alloxan and streptozotocin. Glucose and alloxan are similar mainly in their ring shape. Alloxan acts on many receptors in the body making it highly toxic. Glucose and streptozotocin share a similar ring structure including the inclusion and location of one Oxygen relative to the hydroxyl groups adjacent to the ring and the location of the attached carbon chain. The high conservation of shape between glucose and STZ targets a more specific set of receptors, allowing for a wider dosing range when using STZ.

The use of the STZ mouse model of diabetes is well-established in theory, though in practice many different protocols exist prescribing STZ at varying dosages (55-275 mg/kg) and for varying lengths of time (injections for 1-5 days) [38]. A hyperglycemic diabetic state is generally confirmed by glucose testing of blood recovered through tail snipping. The reported threshold used to classify hyperglycemia is not consistent in literature. In humans the threshold for diagnosis is 11.1 mmol/L (200 mg/dL) or 7 mmol/L (126 mg/dL) when fasting. In mice, the most commonly reported diagnosis threshold is 16 mmol/L or 300 mg/dL if it is reported at all [13].

STZ competes with glucose to enter the β-cell through the Glut2 complex. This specificity is a key aspect of the effectiveness of STZ, and part of the reason why alpha and delta cells in STZ diabetes models behave differently than in autoimmune models. Once inside the cell, the methyl nitrosourea portion of the STZ alkylates DNA, breaking it into fragments. This activates Poly ADP-ribose synthetase to repair the DNA, which in turn depletes the NAD+ supply. NAD+ is crucial to the cellular production of ATP and the lowered ATP production results in the formation of hydrogen peroxide and hydroxyl radicals causing oxidative stress (**Figure 5**). The exact mechanism of cytotoxicity is not understood but death by both necrosis as well as apoptosis have been observed [39].

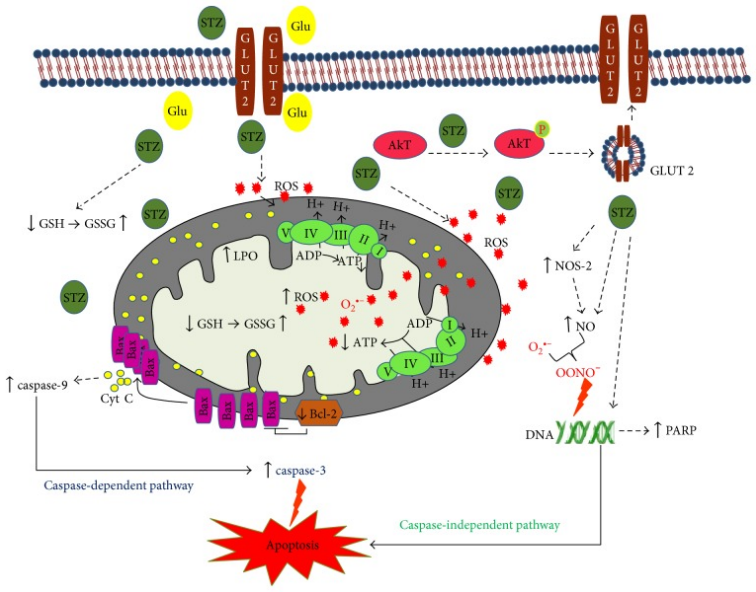

Figure 5. Action of STZ on the cell. STZ enters the cell competitively through the Glut2 complex. STZ causes necrosis and apoptosis, the determining factors of the method by which a cell will expire remain unknown [39].

Although the STZ model has great potential, our lab has been confronted with the effect of estrogen protection in previous attempts to induce diabetes using STZ in female mice. ER-α presents abundantly on the surface of β-islet cells, creating the opportunity for estradiol to intervene in the cellular destruction of STZ by preserving the ability of the mitochondria to produce ATP and by promoting healthy protein production in the endoplasmic reticulum (ER) [40]. The aim of this study was to develop a protocol to reliably induce diabetes in both sexes, as well as to characterize the resulting disease phenotype. Diabetes was successfully induced in all STZ-treated animals and the diabetic mice were characterized by low body weight and bone size, compromised mechanical properties at both the bone and tissue level, and a change in tissue mineral density. The observed changes varied in severity between sexes as the female mice exhibited a more severe deficit in bone strength when compared to the control.

2. MATERIALS AND METHODS

2.1 Mouse Model

Male and female mice purchased from Envigo labs (Indianapolis, IN) were grouped as Control (ctrl) or Treatment (STZ). Mice were weight matched between treatments within each sex (n=15 per group). Mice received intraperitoneal injections of a 50 mM citrate buffer vehicle control or STZ dissolved in the 50 mM citrate buffer (females: 90 mg/kg, males: 65 mg/kg) for 5 consecutive days starting at 8 weeks of age. All mice were sacrificed at 15 weeks of age via cardiac exsanguination, followed by cervical dislocation. Bones were wrapped in gauze soaked in phosphate-buffered saline (PBS) and stored frozen at -20 C.

2.2 Blood Glucose Measurements

Non-fasting blood glucose measurements were made prior to the first STZ injection, and weekly starting one week after the last injection. Blood was collected from the tip of the tail and measured on an Alphatrak 2 glucometer using the mouse setting adjustment prescribed by the manufacturer. (Zoetis Products, Chicago Heights, IL*)*. Blood glucose measurements greater than 300 mg/dL (16.6 mM) were considered to be confirmation of disease.

2.3 Glucose and Insulin Tolerance Testing

Mice were subjected to either glucose tolerance testing (GTT) or insulin tolerance testing (ITT) at 15 weeks of age (n = 7 and n = 8 respectively). Mice in the GTT group were fasted overnight and injected subcutaneously with a bolus of glucose (2 g/kg) at time = 0. The amount of glucose was dependent on the mass of each mouse. Blood glucose measurements were made at 0, 10, 20, 30, 60, and 90 minute timepoints. Data are reported as area under the curve based on averaged values for each group at each timepoint. Mice in the ITT group were fasted for two hours prior to testing. Mice were injected subcutaneously with a bolus of insulin (0.75 U/kg) at time = 0. The amount of insulin was dependent on the mass of each mouse. Blood glucose measurements were made at 15 minute intervals over the course of one hour.

2.4 Pancreatic Analysis

Pancreata were fixed in 10% formalin for 6 hours and embedded in paraffin. For β-cell area, pancreases were processed and immunohistochemistry was performed. Slides were incubated with anti-insulin (C27C9) Rabbit monoclonal antibodies (Cell Signaling Technology, Danvers, MA) overnight at 4°C. Insulin was visualized with anti-rabbit ImmPRESS reagent and NovaRed substrate kit; hematoxylin was used to counterstain tissue. Sections, 3-5 permouse and at least 50 μm apart, were analyzed using Zen Blue software (Zeiss, Oberkochen, Germany). The insulin-positive area in pixels was divided by the total pancreas area in pixels and expressed as a percentage.

2.5 HbA1c Analysis

Between 0.5-1 mL of blood was collected via cardiac exsanguination and stored in EDTA coated tubes. HbA1c was measured using a latex agglutination inhibition assay. Total hemoglobin was determined by conversion to alkaline haematin which has a reliable light absorption spectrum. The reported values are the ratio of the glycated hemoglobin to the total hemoglobin. Measures were performed on a Daytona+ clinical chemistry analyzer (Randox Laboratories, Crumlin, United Kingdom).

2.6 Microcomputed Tomography (μCT)

Right and Left tibiae were scanned through a 0.5 mm aluminum filter (V = 60 kV, I = 167 μA) at a 9.8 per pixel resolution on a Skyscan 1172 (Bruker, Kontich, Belgium). Scans were performed at intervals of 0.7 degrees, averaging two frames at each increment. Scans of hydroxyapatite phantoms (0.25 and 0.75 g/cm^3 CaHA) were used to calibrate bone mineral density. Image reconstruction and rotation was performed in NRecon software (Bruker, Kontich, Belgium) and rotated in DataViewer (Bruker, Kontich, Belgium) to ensure consistent orientation. To analyze geometric properties, 1-mm trabecular regions of interest beginning just distal to the proximal tibial growth plate were segmented from the surrounding cortical shell in CTan software. CTan was then used to measure bone volume fraction (BV/TV), trabecular number (Tb. N), trabecular separation (Tb. Sp), trabecular thickness (Tb. Th), tissue mineral density (TMD), connectivity density, degree of anisotropy, and structure model index (SMI). A 1-mm

cortical region of interest at the tibial mid-diaphysis of each bone was chosen. The geometry of each section was evaluated in a custom Matlab (Mathworks, Natick, MA) script to find total cross-sectional area (TA), bone area (BA), marrow area, bone area fraction (BA/TA), cortical thickness (Ct. Th), moments of inertia along the minor and major axes, and cortical TMD.

2.7 Mechanical Testing

Tibiae were tested to failure in a 4-point bending configuration with a 9 mm support span and a 3 mm loading span. Displacement was applied monotonically in the medial-lateral direction at 0.025 mm/sec (medial surface in tension). Bones were hydrated with phosphate buffered saline (PBS) throughout the test. Force and displacement values were recorded. Analysis was run in Matlab (Mathworks, Natick, MA) to construct a force-displacement curve from which yield force, maximum force, failure force, displacement at yield, post-yield displacement, and total displacement were determined. Stiffness was taken from the linear slope of this curve in the elastic region. Work to yield, post-yield work and total work were calculated from the area underneath the force-displacement curve. Force-displacement data was then normalized with μCT data and mechanical bending equations for four-point bending to produce a stress-strain curve. Yield stress, ultimate stress, failure stress, strain to yield, ultimate strain, and failure strain were identified from this curve and used to calculate the modulus (slope of the stress strain curve), resilience, and toughness (area under the stress-strain curve).

2.8 Fracture Toughness Testing

Prior to fracture toughness testing, right tibiae were scanned via the above μCT protocol. Bones were notched on the anteromedial side distal to the tibial crest to 1/3 of the depth of the bone using a sectioning saw with a 0.003 in thick diamond blade. Bones were kept hydrated throughout testing in three-point bending, utilizing a span of 9.5 mm between supports and a displacement rate of 0.001 mm/s. The notched side of the bone was held in tension. After breaking, marrow was removed from the bones which were then placed in 70%, 80%, 90% and 100% ethanol for 45 minutes each before desiccation overnight. Samples were sputter-coated with gold and imaged via a scanning electron microscope to reveal the angles of crack initiation and instability. These images were combined in a custom MATLAB code with the mechanical

testing data obtained during the fracture to reveal the stress intensities at crack initiation, during the period of crack propagation, and at the final instability fracture.

2.9 Bone AGE Analysis

After mechanical testing, the ends of the broken bones were removed on a Buehler Isomet sectioning saw (Lake Bluff, IL) and marrow was flushed from the marrow cavity. Bones were demineralized for 30 min in Immunocal^{TM} Decalcifier solution (StatLab, McKinney, TX) until clear and pliable. Demineralized bones were rinsed with water, weighed, and dried overnight in an oven at 37C. Samples were transferred to glass hydrolysis tubes and digested with 100 μL 6M HCL/mg at 110C for 20 hours. Samples were cooled, diluted with water, and tested on a Cytation 3 plate reader (Biotek, Winooski, VT) with fluorescence capabilities at 360 nm excitation and 460 nm emission. Samples were tested against a quinine standard and values were normalized to the collagen content of the bone using hydroxyproline as a marker for collagen using a hydroxyproline colorimetric assay kit (BioVision Inc., Milpitas, CA).

2.10 Statistics

Statistics were performed in Prism (GraphPad, Sand Diego, CA). All data were evaluated via 2-way ANOVA testing for main effects of sex and STZ treatment (with $p<0.05$ set as the threshold for statistical significance). If the interaction term from the 2-way ANOVA reached significance, main effects were disregarded and a Tukey's HSD post-hoc analysis was completed. The area under the curve function in prism was first utilized to calculate the value for each GTT and ITT test. These values were then evaluated via 2-way ANOVA. Data are reported as mean +/- standard deviation.

3. RESULTS

3.1 Body mass and tibial length are reduced in diabetic mice

The percent change in mass (change in mass divided by initial mass) was significantly different in the diabetic mice ($P < 0.0001$) (Figure 3, A). Tibial length did not vary with treatment or sex, but post-hoc analyses revealed a significant difference in diabetic vs. healthy female mice, as well as diabetic females vs. diabetic males (Figure 3, B).

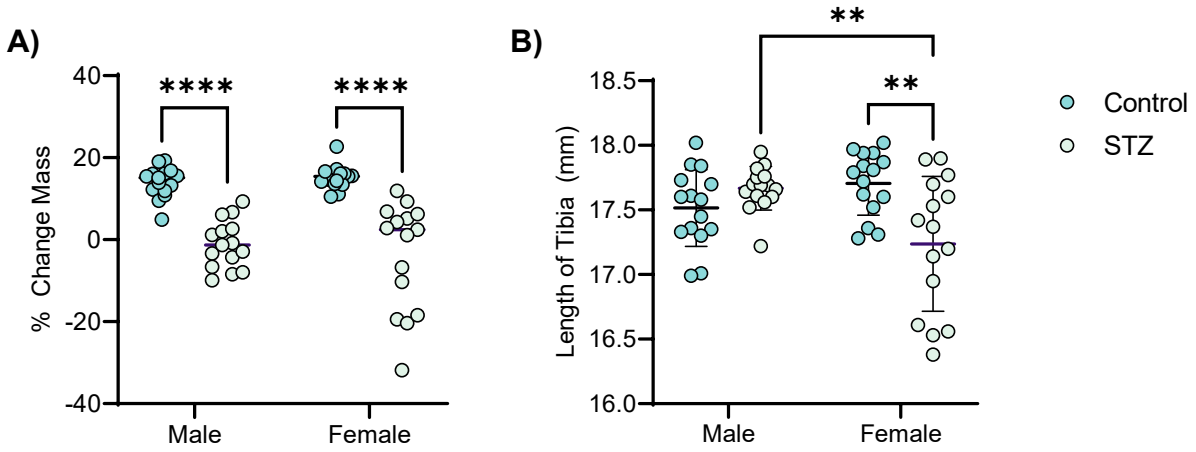

Figure 6. A. Percent change in mass over the timeline of the study. Diabetic mice gained less mass than control mice. **B.** Length of right tibiae at sacrifice. The tibiae of diabetic males were not significantly different in length versus those of the control males. The right tibiae of the female mice were shorter than those of the control tibiae in 50% of treated mice, a significant difference was present between female disease and healthy groups. All data are presented as mean +/- SD.

3.2 Glucose tolerance is impaired in diabetic mice

To evaluate glucose tolerance and assess β-cell function, a glucose tolerance test (GTT) was performed. As expected, mice treated with STZ had significantly worsened glucose tolerance. No differences were noted between males and females. ($P < 0.0001$, **Figure 7**).

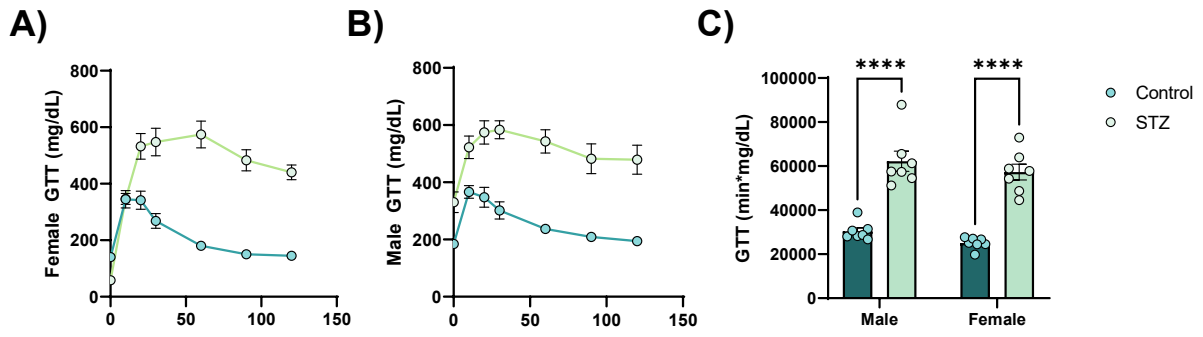

Figure 7. Glucose Tolerance Results. **A.** Control female mice began to breakdown injected glucose within 10 minutes of injection, returning close to pre-injection levels after one hour. Diabetic females did not begin to metabolize glucose within the first hour after injection, levels did not return to pre-injection during the time-course of the observation. **B.** Control male mice began to breakdown injected glucose within 10 minutes of injection, returning close to pre-injection levels after one hour. Diabetic males did not begin to metabolize glucose until the 45 minute mark. Glucose levels did not return to pre-injection during the time-course of the observation.. **C.** There was a significant difference between the ability of control and diabetic mice to modulate the injected glucose. Data presented as mean +/- SEM. **** indicates p<0.0001

In healthy animals, blood glucose spiked and peaked within the first 10 minutes of observation. The glucose in the diabetic mice continued to climb, peaking around 30 minutes for the males and around 1 hour for the females. Control mice rapidly returned to the fasting blood glucose level, fully recovering within the first hour. Treated mice did not begin to process the glucose as quickly, and never returned to their fasting blood glucose levels. There was no significant difference between healthy males and females or the diabetic males and females.

3.3 Insulin tolerance is impaired in diabetic mice

Blood glucose levels were measured every 15 minutes for the 60-minute period following an insulin injection. There was a significant difference in the ability to tolerate this insulin injection between control and treated animals ($p<0.0001$, **Figure 8**).

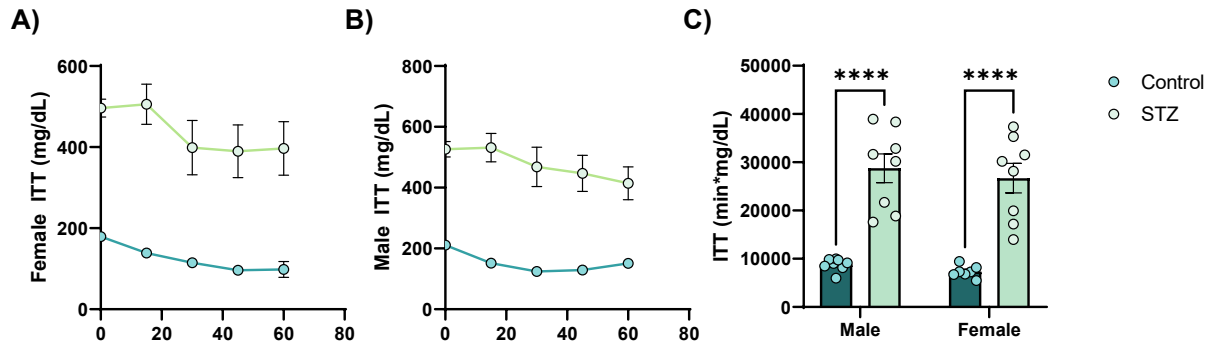

Figure 8. Insulin Tolerance Results. **A.** Control female mice experienced a near immediate reduction in blood glucose which continued for the full hour of observation. Diabetic females experienced an immediate increase in glucose, followed by a sharp drop between 10 and 30 minutes of observation. The reduction in blood glucose did not reach healthy levels, remaining in the hyperglycemic range for the duration of the experiment. **B.** Control male mice exhibited the same early drop in blood glucose, after a half hour, blood-glucose levels began to return to pre-injection levels. Diabetic males did not respond immediately, experiencing a slight increase in glucose at the 15 minute mark. The diabetic male glucose levels decreased steadily for the remainder of the observation period. **C.** There was a significant difference between the ability of control and diabetic mice to process the injected insulin. Data presented as mean +/- SEM. *** indicates $p<0.0001$.

The glucose level of the control animals began to decrease within the first time segment, while the diabetic animals experienced a small spike in blood glucose 15 minutes post injection **(Figure 8**). Between 15 and 30 minutes, blood glucose of the diabetic animals began to drop. By the end of the hour, blood glucose of the diabetic animals was lower than pre-injection, although within the period of observation blood glucose never dropped low enough to bring the mice out of a hyperglycemic state. There was no significant difference between the sexes.

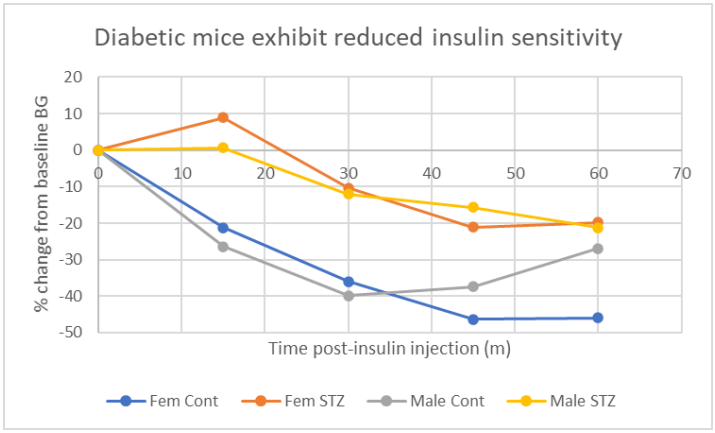

Figure 9. Percent change blood glucose level after treatment with exogenous insulin. Diabetic mice exhibited lower insulin sensitivity than control counterparts.

3.4 Female diabetic mice lose beta cell mass after diabetes induction

The pancreata of treated mice had significantly lower beta cell area, a proxy measurement for beta cell mass, versus the control group (P = 0.0014, **Figure 9**). There was no significant difference between sexes.

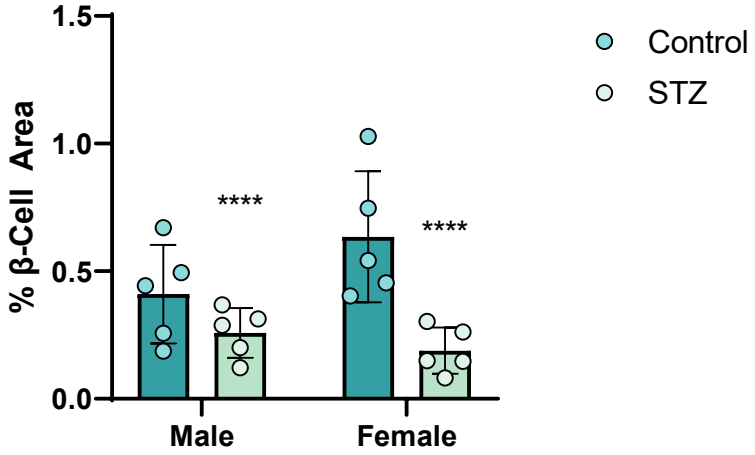

Figure 10. Percent β-cell area. Diabetic mice had a significantly less beta-cell area when compared to healthy counterparts (**** indicates p = 0.0014). Data presented as mean +/- SD.

3.5 Glycated hemoglobin is increased in diabetic mice

A value of 4% HbA1c, a measure of the average percent of glycated hemoglobin in the blood of healthy mice was established (**Figure 10**). In both sexes, diabetic mice had roughly double the HbA1c level in their blood compared with their healthy counterparts (P < 0.0001). HbA1c was also higher in males versus females (P = 0.0160).

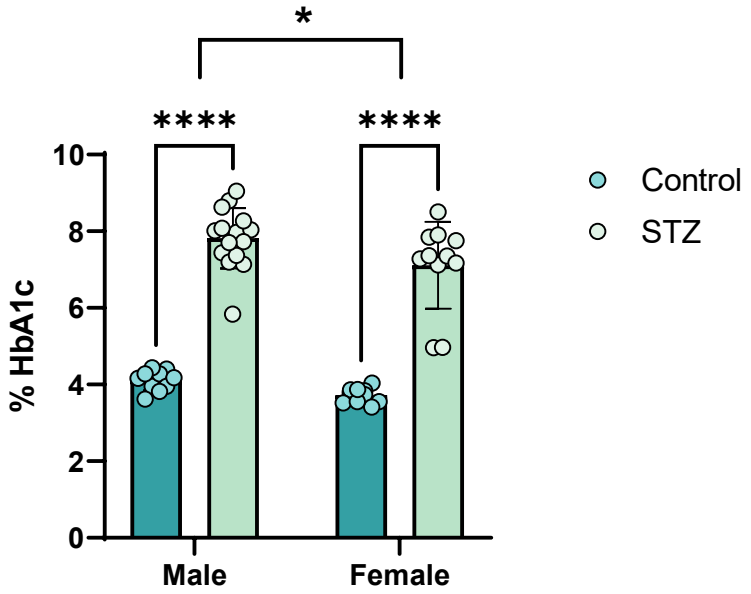

Figure 11. Percent glycated hemoglobin in plasma. Diabetic mice had significantly higher amounts of glycated hemoglobin compared to healthy mice (**** indicates p<0.0001). Female mice had significantly less glycated hemoglobin than males in comparisons between healthy mice of different sexes and diabetic mice of different sexes (* indicates p = 0.0160). Data presented as mean +/- SD.

3.6 Fluorescent AGEs were not altered in diabetic mice

Mice tibiae were evaluated for presence of AGEs using an assay sensitive to the fluorescent nature of most AGEs. This could indicate a change in the frequency of non-enzymatic glycation events within the bone. There were no significant differences in the levels of fluorescence measured across the groups (**Figure 11**).

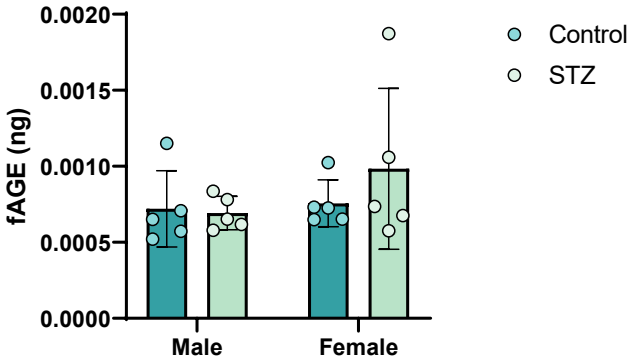

Figure 12. Fluorescence of advanced glycation end products. There was no significant difference in the amount of fAGEs in the control or treated animals. Data presented as mean +/- SD.

3.7 Cancellous bone morphology is altered

Diabetic mice had lower tissue mineral density and degree of anisotropy compared with their control counterparts (**Table 2**). Diabetic females had thinner trabeculae than the control females. There was a strong sexual dimorphism in the control animals which persisted through the disease state for all trabecular properties with the exception of degree of anisotropy and structure model index (SMI). The trabecular number, thickness and connectivity density were lower in the female animals versus the males, while the trabecular separation was greater. This contributed to a lower overall bone volume fraction in female groups. Tissue mineral density was also significantly lower in the females vs. the males.

Table 2. Properties of trabecular bone from microcomputed tomography. Significant P- Values indicated in bold in columns on right. Post-hoc significance indicated as: [a] significance compared to male control, [b] significance compared to female control, [c] significance compared to male STZ, [d] significance compared to female STZ, [†] significance of disease within sex. Data represented as mean +/- SD.

	MALE		FEMALE		P-Value from Two-way ANOVA		
	CONTROL (n=15)	STZ (n=15)	CONTROL (n=15)	STZ (n=15)	Disease	Sex	Interaction
Bone Volume Fraction (%)	14.7 ± 2.45	13.66 ± 1.83	11.46 ± 1.68	10.87 ± 1.09	0.1035	**<0.0001**	0.6502
Trabecular Thickness (mm)	0.058 ± 0.00 [b]	0.055 ± 0.00 [b]	0.062 ± 0.00 [a,c,d]	0.055 ± 0.00 [b]	**<0.0001**	**0.0144**	**0.0255**
Trabecular Number (1/mm)	2.55 ± 0.45	2.48 ± 0.31	1.86 ± 0.27	1.98± 0.20	0.806	**<0.0001**	0.2853
Trabecular Separation (mm)	0.187 ± 0.014	0.195 ± 0.013	0.272 ± 0.04	0.259 ± .258	0.7148	**<0.0001**	0.1375
TMD (g/cm^3)	0.75 ± 0.01	0.73 ± 0.02	0.77 ± 0.02	0.75 ± 0.03	**0.0002**	**0.0038**	0.8723
Degree of Anisotropy	2.58 ± 0.18	2.42 ± 0.24	2.70 ± 0.34	2.27 ± 0.21	**<0.0001**	0.8216	0.0558
SMI	2.06 ± 0.19	2.02 ± 0.13	2.11 ± 0.09	2.04 ± 0.11	0.1032	0.379	0.7322
Connectivity Density (1/mm^3)	168.97 ± 48.34	178.78 ± 64.94	129.00 ± 31.07	134.61 ± 20.39	0.5197	**0.0008**	0.8604

3.8 Cortical geometry differs between male and female mice

At the tibial mid-diaphysis, marrow area was increased while cortical area, bone area fraction, and tissue mineral density were reduced in diabetic mice from both sexes (**Table 3**). The moment of inertia about the major axis was smaller in the females than in the males but was consistent between diabetic and healthy groups. There was a significant interaction between sex and disease for total bone area. Post-hoc testing revealed there was no statistical difference between the diabetic and healthy groups in either sex. There was also an interaction for moment of inertia about the minor axis. Post-hoc testing showed a significant difference between diabetic and healthy females.

Table 3. Properties of cortical bone from microcomputed tomography. Significant P- Values indicated in bold in columns on right. Post-hoc significance indicated as: [a] significance compared to male control, [b] significance compared to female control, [c] significance compared to male STZ, [d] significance compared to female STZ, [†] significance of disease within sex. Data represented as mean +/- SD.

	MALE		FEMALE		P-Value from Two-way ANOVA		
	CONTROL (n=15)	STZ (n=15)	CONTROL (n=15)	STZ (n=15)	Disease	Sex	Interaction
Total Area (mm^2)	1.14 ± 0.1^{d}	$1.19 \pm 0.15^{b,d}$	1.04 ± 0.1^{c}	$0.95 \pm 0.11^{a,c}$	0.5479	**<0.0001**	**0.0407**
Marrow Area (mm^2)	0.45 ± 0.04	0.52 ± 0.1	0.38 ± 0.05	0.41 ± 0.08	**0.0091**	**<0.0001**	0.2646
Cortical Area (mm^2)	0.69 ± 0.06^{d}	0.67 ± 0.06^{d}	$0.65 \pm 0.05^{\dagger}$	$0.54 \pm 0.06^{\dagger}$	**<0.0001**	**<0.0001**	**0.0085**
Bone Area Fraction	60.87 ± 1.21	56.51 ± 3.38	63.34 ± 1.84	57.06 ± 4.51	**<0.0001**	0.0669	0.2382
Cortical Thickness	0.22 ± 0.01	0.21 ± 0.01	0.22 ± 0.01	0.19 ± 0.02	0.8205	0.1912	0.1642
Imax (mm^4)	0.12 ± 0.04	0.12 ± 0.05	0.09 ± 0.04	0.07 ± 0.03	0.9177	**0.0328**	0.9177
Imin (mm^4)	0.08 ± 0.01^{d}	0.08 ± 0.01^{d}	$0.07 \pm 0.01^{\dagger}$	$0.05 \pm 0.01^{\dagger,a,c}$	**0.0264**	**<0.0001**	**0.004**
Cortical TMD	1.33 ± 0.04	1.29 ± 0.06	1.33 ± 0.05	1.36 ± 0.04	**0.0003**	0.1069	0.1028

3.9 The mechanical strength of female mice is altered in STZ-induced diabetes

Although there were significant main effects of disease for yield force, maximum force, failure force, and stiffness, these comparisons were complicated by significant interactions (**Figure 12, Table 4**).

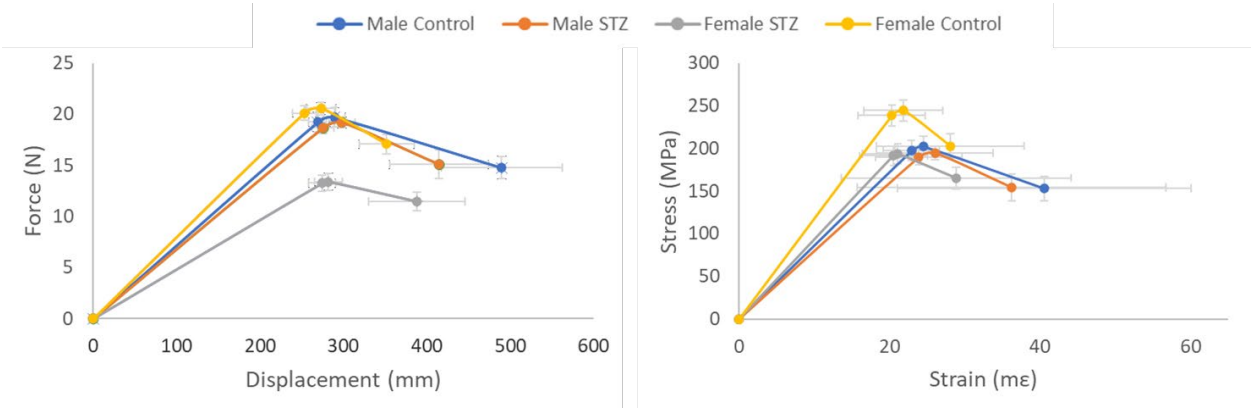

Figure 13. Control bones withstood more maximum force than diabetic bones, with female bones exhibiting the greatest difference. The control bones withstood higher stresses than the diabetic bones while experiencing similar amounts of strain. Data presented as mean +/- SEM.

Post-hoc evaluation revealed significance of disease in female mice only with all properties being lower in diseased versus control mice. There were significant main effects of sex for yield force, maximum force, and work to yield, but these were again complicated by significant interactions. Post-hoc testing showed a difference of sex in healthy mice but not in diseased

mice. In both diabetic and healthy mice there was no significant difference in displacement values during testing.

Table 4. Values calculated from force-displacement data. Significant P- Values indicated in bold in columns on right. Post-hoc significance indicated as: [a] significance compared to male control, [b] significance compared to female control, [c] significance compared to male STZ, [d] significance compared to female STZ, [†] significance of disease within sex. Data represented as mean +/- SD.

	MALE		FEMALE		P-Value from Two-way ANOVA		
	CONTROL (n=15)	STZ (n=15)	CONTROL (n=15)	STZ (n=15)	Disease	Sex	Interaction
Yield Force (N)	19.22 ± 3.59[b]	18.66 ± 2.18[b]	20.1 ± 2.59[†,a,c]	13.25 ± 2.95[†]	**0.0001**	**0.0046**	**<0.0001**
Maximum Force (N)	19.70 ± 3.52 [b]	19.18 ± 1.89 [b]	20.54 ± 2.23[†,a,c]	13.39 ± 3.09[†]	**<0.0001**	**0.0015**	**<0.0001**
Failure Force (N)	14.78 ± 4.14	15.09 ± 5.32	17.07 ± 3.68[†]	11.47 ± 3.37[†]	**0.0109**	0.5551	**0.0218**
Displacement to Yield (µm)	268.91 ± 39.86	275.37 ± 49.65	253.07 ± 51.63	274.36 ± 59.01	0.5851	0.5351	0.3084
Postyield Displacement (µm)	220.67 ± 246.66	138.8 ± 234.76	98.33 ± 98.42	113.60 ± 206.24	0.3793	0.1837	0.5459
Total Displacement (µm)	489.58 ± 270.72	414.17 ± 221.75	351.41 ± 123.00	387.96 ± 215.66	0.3331	0.1573	0.736
Stiffness (N/mm)	78.19 ± 14.03[d]	74.15 ± 11.74[b,d]	90.54 ± 20.8[†,c]	53.65 ± 12.1[†,a,b]	**<0.0001**	0.3169	**0.0002**
Work to Yield (mJ)	2.81 ± 0.75[b]	2.77 ± 0.72[b]	2.75 ± 0.6[†,a,c]	2.00 ± 0.65[†]	0.0562	**0.0266**	**0.0328**
Postyield Work (mJ)	3.4 ± 3.47	1.6 ± 2.04	1.37 ± 2.36	1.65 ± 1.43	0.2483	0.1345	0.1163
Total Work (mJ)	6.21 ± 3.91[b]	4.37 ± 1.86	3.37 ± 2.57[a]	4.4 ± 1.65	0.5697	0.0521	**0.0468**

3.10 Diabetic bones of females are less able to absorb energy prior to fracture

At the tissue level, female disease bones deformed under significantly less stress than the female control bones as was indicated by significantly lower yield and maximum stresses (**Table 5**). This was reflected in the calculation of a lower elastic modulus for the disease females. The sexual dimorphism inherent in the skeleton persisted at the tissue level where female bones failed at significantly lower stress and withstood less strain to yield and at failure than male bones. This again led to a lower overall modulus of elasticity.

Table 5. Values calculated from mechanical testing data, μCT data and three-point bending equations. Significant P-Values indicated in bold in columns on right. Post-hoc significance indicated as: [a] significance compared to male control, [b] significance compared to female control, [c] significance compared to male STZ, [d] significance compared to female STZ, [†] significance of disease within sex. Data represented as mean +/- SD.

	MALE		FEMALE		P-Values from Two-way ANOVA		
	CONTROL (n=15)	STZ (n=15)	CONTROL (n=15)	STZ (n=15)	Disease	Sex	Interaction
Yield Stress (MPa)	197.19 ± 43.78	189.57 ± 33.37[d]	238.54 ± 45.49[†]	191.17 ± 42.06[c,†]	0.0781	0.0575	**0.0161**
Maximum Stress (MPa)	202.12 ± 43.30[d]	194.52 ± 30.44[d]	244.48 ± 46.08[†]	193.39 ± 45.12[†,a,c,]	0.0562	0.0698	**0.011**
Failure Stress (MPa)	153.03 ± 53.10	154.14 ± 60.54	202.75 ± 53.24	165.19 ± 46.84	0.1829	**0.0385**	0.2089
Strain to Yield (mε)	22.881 ± 3.761	23.855 ± 5.730	20.282 ± 4.467	20.518 ± 4.525	0.7685	**0.021**	0.6302
Ultimate Strain (mε)	24.498 ± 3.845	26.030 ± 7.762	21.823 ± 5.261	21.083 ± 4.729	0.4504	**0.0135**	0.7919
Failure Strain (mε)	40.550 ± 19.543	36.232 ± 20.512	28.070 ± 9.830	28.828 ± 15.281	0.5747	**0.0312**	0.6937
Modulus (GPa)	9.72 ± 2.71 [d]	8.88 ± 1.94 [d]	13.71 ± 4.26[†]	10.48 ± 2.57[†,a,c,]	0.1445	**0.001**	**0.0134**
Resilience (MPa)	2.39 ± 0.57	2.42 ± 0.72	2.17 ± 0.75	2.59 ± 0.57	0.2063	0.8746	0.2769
Toughness (MPa)	5.20 ± 3.07	3.80 ± 1.74	3.69 ± 2.97	4.15 ± 1.54	0.4732	0.3788	0.1581

3.11 Fracture Toughness

Fracture toughness testing measures the stress intensity at crack initiation, maximum load, and fracture instability. There was no significant difference between the sexes. The only significant difference noted was a decrease in fracture instability toughness with disease, an indication of reduced fracture resistance (P=0.0409).

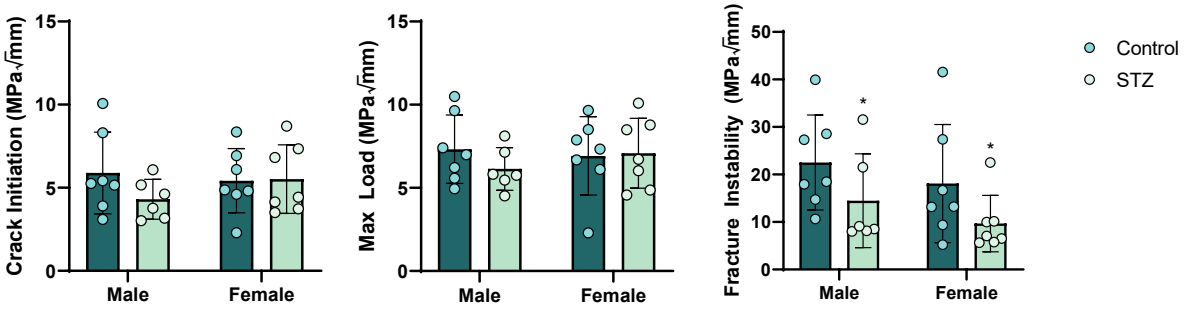

Figure 14. Fracture Toughness Testing. In all groups crack initiation and maximum load happened at similar intensities. Diabetic fractured at lower intensities than control bones. * indicates p<0.0409. Data presented as mean +/- SD.

4. DISCUSSION

The successful induction of a model of Type 1 diabetes in both sexes was indicated by persistent high glucose in the blood, reduced insulin tolerance, elevated HbA1c levels and change in mass. However, the differences in bone were more compelling in the female mice.

Diabetic mice were significantly smaller at the end of the study than their previously weight and sex matched counter cohorts. Although mice continued to eat throughout the study this did not translate to weight gain. As the ability to use insulin to convert glucose to energy was lost, the mice may have begun to metabolize adipose tissue within the body, losing weight, a common side effect of diabetes [10]. In females, tibial length of the treated cohort was significantly shorter than the tibial length of the control cohort. The most striking difference is the wide distribution of lengths and weights among diabetic females. The lengths of the control animals were tightly grouped, representing the average size for 15 wk old healthy females. Only half of the treated female lengths fell within this range, with the other half being shorter. This was not replicated in the males, where a significant decrease in both weight and tibial length was observed, all within a small range compared to the disparity in the female values.

Anecdotally, the female mice continued to climb and attempt to evade capture through the end of the study while males were observed to be lethargic, huddling in the cage rather than running or climbing. It could be expected that in the case of greater mechanical loading during growth, the female might experience increased growth due to the loading stimulation. This was not the case, suggesting that the reduction in bone length is not a result of reduced loading stimulus as animals became ill but rather the result of the compromised bone maintenance and growth. This is supported by the mechanical testing data. Stress-strain data is normalized for bone size so the significant decrease in stress, absent a significant change in strain which resulted in a reduced elastic modulus indicates the bone is in a more brittle state. This is likely caused by the addition of non-enzymatic bonds in collagen. The compromised ability of the diabetic bones to resist crack propagation during fracture toughness testing further support the reduction in bone quality. This increased brittleness may be a result of undetected AGE binding.

Interestingly, the female mice experienced more severe outcomes than the males in the majority of parameters. While development of a protocol to induce diabetes in the females was difficult, once the protective effects of estrogen on the pancrease were overcome the effects on

the bones were more comprehensive than in the male bones. A future look at serum estrogen levels in mice may give insight into the interplay between the estrogen and the streptozotocin-treated mouse. Understanding the relationship between glucose, estrogen, and bone may inform diabetes and non-diabetic osteoporotic bone research alike.

The sexual dimorphism in disease presentation does not extend to the blood and pancreas related parameters. Glucose tolerance testing showed that while the healthy mice were able to produce insulin to metabolize a bolus of glucose, the diabetic mice were not able to reduce blood glucose back down to pre-injection levels. Insulin tolerance testing revealed that the diabetic mice also lacked the ability to utilize exogenous insulin to recover their blood glucose to a healthy level. This was further supported by other work in this lab where an attempt was made to treat diabetic males with insulin pellets implanted under the skin. The mice experienced lower glucose in the short term but ultimately glucose levels rose regardless of insulin treatment. The lack of ability to produce and metabolize insulin is not a direct match for a human T1D disease state though it is similar to the combined autoimmune and insulin resistance exhibited by 30% of the diabetic population [9, 16].

The increase in glycated hemoglobin in the blood of diabetic mice mirrors the results of HbA1c plasma testing in humans. HbA1c is preferred over fasting glucose because it provides a look at the glycemic within the last period of red blood cell turnover, roughly 120 days in humans and 45 days in C57/BL6 mice [41, 42]. Males experienced significantly higher levels of glycation than females, an observation consistent with reports of HbA1c levels in humans with T1D, but without explanation [38, 43]. There is evidence that this difference may be reversed in T2D patients, where females reportedly have higher levels of HbA1c than males and there is no record of the trend in patients exhibiting both loss of insulin production and resistance to insulin [34]. This is an area for future study to determine the connection between sex and HbA1c levels in diabetes. Other work by our lab has shown that allowing the diabetic state to persist longer results in higher %HbA1c values in diabetic mice. This supports the idea that glycation will increase over time, resulting in a more profound disease state with secondary complications.

It was hypothesized that one such complication would be the existence of increased AGEs within the bone tissue which would lead to a stiffening of the collagen matrix [25]. Although fluorescent AGE testing in bone did not bear this out, there are several reasons why this does not discount the hypothesis. The most abundant AGE in bone is carboxymethyl-lysine (CML), which

does not fluoresce and therefore may exist in the diabetic bones undetected by our fluorescence detection methods but potentially measurable through ELISA [28]. Additionally, while the hemoglobin exists within the sugar-saturated blood, increased glucose likely takes longer to infiltrate the interstitial fluid in the bone. Given more time it is likely the bones would experience a measurable increase in AGE binding driving a decrease in bone ductility and producing a more compelling bone phenotype.

The young age of induction of these mice was chosen to attempt to overcome the inability of researchers to induce diabetes in the adult females, a caveat being that the mice were potentially able to recover some bone damage due to the higher level of cellular activity in young bones. At the same time, the impaired growth and weight gain presents a challenge for continuing to study these mice through adulthood. Using the developed protocol but inducing at a point in which the bones have had a chance to mature further may provide a chance to explore the longer-term effects of the disease.

The development of a protocol to reliably induce diabetes in both sexes was successful, with 100% of the mice crossing the glucose threshold for diabetes and surviving the duration of the study. The mice experienced reduced bone mineral density, compromised bone quality, and reduced growth in keeping with clinical diabetic outcomes [26]. The ability of this model to mimic human symptoms of diabetes, as well as the presentation of a strong bone disease phenotype, makes the STZ-induced diabetic mouse a good candidate for future work in the study of diabetes and bone.

REFERENCES

1. R. Bouillon *et al.*, "Skeletal and Extraskeletal Actions of Vitamin D: Current Evidence and Outstanding Questions," *Endocr Rev,* vol. 40, no. 4, pp. 1109-1151, Aug 1 2019, doi: 10.1210/er.2018-00126.
2. E. S. Vasiliadis, T. B. Grivas, and A. Kaspiris, "Historical overview of spinal deformities in ancient Greece," *Scoliosis,* vol. 4, p. 6, Feb 25 2009, doi: 10.1186/1748-7161-4-6.
3. B. Cooper, "The origins of bone marrow as the seedbed for our blood: from antiquity to the time of Osler," *Proceedings: Baylor University Medical Center,* vol. 24, 2, p. 3, 2011.
4. Y. Han, X. You, W. Xing, Z. Zhang, and W. Zou, "Paracrine and endocrine actions of bone-the functions of secretory proteins from osteoblasts, osteocytes, and osteoclasts," *Bone Res,* vol. 6, p. 16, 2018, doi: 10.1038/s41413-018-0019-6.
5. X. Feng, "Chemical and Biochemical Basis of Cell-Bone Matrix Interaction in Health and Disease," *Curr Chem Biol,* vol. 3, no. 2, pp. 189-196, May 1 2009, doi: 10.2174/187231309788166398.
6. N. Li *et al.*, "An Updated Systematic Review of Cost-Effectiveness Analyses of Drugs for Osteoporosis," *Pharmacoeconomics,* vol. 39, no. 2, pp. 181-209, Feb 2021, doi: 10.1007/s40273-020-00965-9.
7. E. Stein and E. Shane, "Secondary osteoporosis," *Endocrinology and Metabolism Clinics of North America,* vol. 32, no. 1, pp. 115-134, 2003, doi: 10.1016/s0889-8529(02)00062-2.
8. S. Khosla, M. J. Oursler, and D. G. Monroe, "Estrogen and the skeleton," *Trends Endocrinol Metab,* vol. 23, no. 11, pp. 576-81, Nov 2012, doi: 10.1016/j.tem.2012.03.008.
9. J. Khawandanah, "Double or hybrid diabetes: A systematic review on disease prevalence, characteristics and risk factors," *Nutr Diabetes,* vol. 9, no. 1, p. 33, Nov 4 2019, doi: 10.1038/s41387-019-0101-1.
10. G. Wilcox, "Insulin and insulin resistance," *The Clinical Biochemist,* vol. 26, 2, p. 20, 2005.
11. J. Starup-Linde, K. Hygum, T. Harslof, and B. Langdahl, "Type 1 Diabetes and Bone Fragility: Links and Risks," *Diabetes Metab Syndr Obes,* vol. 12, pp. 2539-2547, 2019, doi: 10.2147/DMSO.S191091.
12. D. R. Weber, K. Haynes, M. B. Leonard, S. M. Willi, and M. R. Denburg, "Type 1 diabetes is associated with an increased risk of fracture across the life span: a population-based cohort study using The Health Improvement Network (THIN)," *Diabetes Care,* vol. 38, no. 10, pp. 1913-20, Oct 2015, doi: 10.2337/dc15-0783.
13. L. A. DiMeglio, C. Evans-Molina, and R. A. Oram, "Type 1 diabetes," *The Lancet,* vol. 391, no. 10138, pp. 2449-2462, 2018, doi: 10.1016/s0140-6736(18)31320-5.

14. S. Fazeli Farsani, P. C. Souverein, M. M. J. van der Vorst, C. A. J. Knibbe, A. de Boer, and A. K. Mantel-Teeuwisse, "Chronic comorbidities in children with type 1 diabetes: a population-based cohort study," *Archives of Disease in Childhood,* vol. 100, pp. 763-768, 2015-08-01 00:00:00 2015.

15. D. Dabelea *et al.*, "Trends in the prevalence of ketoacidosis at diabetes diagnosis: the SEARCH for diabetes in youth study," *Pediatrics,* vol. 133, no. 4, pp. e938-45, Apr 2014, doi: 10.1542/peds.2013-2795.

16. N. Kietsiriroje, S. Pearson, M. Campbell, R. A. S. Ariens, and R. A. Ajjan, "Double diabetes: A distinct high-risk group?," *Diabetes Obes Metab,* vol. 21, no. 12, pp. 2609-2618, Dec 2019, doi: 10.1111/dom.13848.

17. N. H. Cho *et al.*, "IDF Diabetes Atlas: Global estimates of diabetes prevalence for 2017 and projections for 2045," *Diabetes Res Clin Pract,* vol. 138, pp. 271-281, Apr 2018, doi: 10.1016/j.diabres.2018.02.023.

18. K. Karastergiou, S. R. Smith, A. S. Greenberg, and S. K. Fried, "Sex Differences in Human Adipose Tissues - The Biology of Pear Shape," *Biology of Sex Differences,* 2012.

19. A. Kautzky-Willer, J. Harreiter, and G. Pacini, "Sex and Gender Differences in Risk, Pathophysiology and Complications of Type 2 Diabetes Mellitus," *Endocr Rev,* vol. 37, no. 3, pp. 278-316, Jun 2016, doi: 10.1210/er.2015-1137.

20. I. Nookaew *et al.*, "Adipose tissue resting energy expenditure and expression of genes involved in mitochondrial function are higher in women than in men," *J Clin Endocrinol Metab,* vol. 98, no. 2, pp. E370-8, Feb 2013, doi: 10.1210/jc.2012-2764.

21. X. Chen, R. McClusky, Y. Itoh, K. Reue, and A. P. Arnold, "X and Y chromosome complement influence adiposity and metabolism in mice," *Endocrinology,* vol. 154, no. 3, pp. 1092-104, Mar 2013, doi: 10.1210/en.2012-2098.

22. B. Tramunt *et al.*, "Sex differences in metabolic regulation and diabetes susceptibility," *Diabetologia,* vol. 63, no. 3, pp. 453-461, Mar 2020, doi: 10.1007/s00125-019-05040-3.

23. C. Le May *et al.*, "Estrogens protect pancreatic beta cells from apoptosis and prevent insulin-deficient diabetes mellitus in mice," *PNAS,* vol. 103, no. 24, p. 6, 2006, doi: 10.1073/pnas.0602956103.

24. N. Napoli *et al.*, "Mechanisms of diabetes mellitus-induced bone fragility," *Nat Rev Endocrinol,* vol. 13, no. 4, pp. 208-219, Apr 2017, doi: 10.1038/nrendo.2016.153.

25. H. Z. Meng, W. L. Zhang, F. Liu, and M. W. Yang, "Advanced Glycation End Products Affect Osteoblast Proliferation and Function by Modulating Autophagy Via the Receptor of Advanced Glycation End Products/Raf Protein/Mitogen-activated Protein Kinase/Extracellular Signal-regulated Kinase Kinase/Extracellular Signal-regulated Kinase (RAGE/Raf/MEK/ERK) Pathway," *J Biol Chem,* vol. 290, no. 47, pp. 28189-28199, Nov 20 2015, doi: 10.1074/jbc.M115.669499.

26. V. Sundararaghavan, M. M. Mazur, B. Evans, J. Liu, and N. A. Ebraheim, "Diabetes and bone health: latest evidence and clinical implications," *Ther Adv Musculoskelet Dis,* vol. 9, no. 3, pp. 67-74, Mar 2017, doi: 10.1177/1759720X16687480.

27. M. Nakamura, S. Nagafuchi, K. Yamaguchi, and R. Takaki, "The Role of Thymic Immunity and Insulitis in the development of Streptozotocin-induced Diabetes in Mice," *Diabetes,* vol. 3, 1984.

28. S. Y. Goh and M. E. Cooper, "Clinical review: The role of advanced glycation end products in progression and complications of diabetes," *J Clin Endocrinol Metab,* vol. 93, no. 4, pp. 1143-52, Apr 2008, doi: 10.1210/jc.2007-1817.

29. L. Gennari *et al.*, "Circulating sclerostin levels and bone turnover in type 1 and type 2 diabetes," *J Clin Endocrinol Metab,* vol. 97, no. 5, pp. 1737-44, May 2012, doi: 10.1210/jc.2011-2958.

30. P. Vestergaard, "Discrepancies in bone mineral density and fracture risk in patients with type 1 and type 2 diabetes--a meta-analysis," *Osteoporos Int,* vol. 18, no. 4, pp. 427-44, Apr 2007, doi: 10.1007/s00198-006-0253-4.

31. Z. Rahimi, "Parathyroid Hormone, glucose metabolism and diabetes mellitus," *Journal of Parathyroid Disease,* p. 2.

32. L. Kahanovitz, P. M. Sluss, and S. J. Russell, "Type 1 Diabetes - A Clinical Perspective," *Point Care,* vol. 16, no. 1, pp. 37-40, Mar 2017, doi: 10.1097/POC.0000000000000125.

33. T. Du, G. Yuan, X. Zhou, and X. Sun, "Sex differences in the effect of HbA1c-de fi ned diabetes on a wide range of cardiovascular disease risk factors," *Ann Med,* vol. 48, no. 1-2, pp. 34-41, 2016, doi: 10.3109/07853890.2015.1127406.

34. G. D. F *et al.*, "Sex differences and correlates of poor glycaemic control in type 2 diabetes: a cross-sectional study in Brazil and Venezuela," *BMJ Open,* vol. 9, no. 3, p. e023401, Mar 5 2019, doi: 10.1136/bmjopen-2018-023401.

35. A. J. King, "The use of animal models in diabetes research," *Br J Pharmacol,* vol. 166, no. 3, pp. 877-94, Jun 2012, doi: 10.1111/j.1476-5381.2012.01911.x.

36. J. W. Yoon, and Jun, H.S., "Cellular and Molecular Pathogenic Mechanisms of Insulin-Dependant Diabetes Mellitus," *Annals of the New York Academy of Sciences,* vol. 928, no. 1, p. 11, 2006.

37. O. M. Ighodaro, A. M. Adeosun, and O. A. Akinloye, "Alloxan-induced diabetes, a common model for evaluating the glycemic-control potential of therapeutic compounds and plants extracts in experimental studies," *Medicina (Kaunas),* vol. 53, no. 6, pp. 365-374, 2017, doi: 10.1016/j.medici.2018.02.001.

38. C. Chandramouli *et al.*, "Diastolic dysfunction is more apparent in STZ-induced diabetic female mice, despite less pronounced hyperglycemia," *Sci Rep,* vol. 8, no. 1, p. 2346, Feb 5 2018, doi: 10.1038/s41598-018-20703-8.

39. A. M. T. A. Nahdi, A. John, and H. Raza, "Elucidation of Molecular Mechanisms of Streptozotocin-Induced Oxidative Stress, Apoptosis, and Mitochondrial Dysfunction in Rin-5F Pancreatic β-Cells," *Oxidative Medicine and Cellular Longevity,* vol. 2017, p. 7054272, 2017/08/06 2017, doi: 10.1155/2017/7054272.

40. A. A. Gupte, H. J. Pownall, and D. J. Hamilton, "Estrogen: An Emerging Regulator of Insulin Action and Mitochondrial Function," *Journal of Diabetes Research,* vol. 2015, p. 916585, 2015/03/26 2015, doi: 10.1155/2015/916585.

41. U. Dholakia, S. Bandyopadhyay, E. A. Hod, and K. A. Kevin A Prestia, "Determination of RBC Survival in C57BL/6 and C57BL/6-Tg (UBC-GFP) Mice," *Comparative Medicine,* vol. 65, 3, p. 5, 2015.

42. V. L. Lew and T. Tiffert, "On the Mechanism of Human Red Blood Cell Longevity: Roles of Calcium, the Sodium Pump, PIEZO1, and Gardos Channels," *Front Physiol,* vol. 8, p. 977, 2017, doi: 10.3389/fphys.2017.00977.

43. B. Tramunt *et al.*, "Sex differences in metabolic regulation and diabetes susceptibility," *Diabetologia,* vol. 63, no. 3, pp. 453-461, 2020/03/01 2020, doi: 10.1007/s00125-019-05040-3.